Measurement and Theoretical Modeling of the Damping Rate of Medium-n Toroidal Alfvén Eigenmodes in JET

D.Testa[1], T.Panis[1], A.Fasoli[1], P.Blanchard[1,2], H.Carfantan[3], A.Goodyear[4], N.Mellet[1,5], S.E.Sharapov[4], D.Spong[6], JET-EFDA contributors*

JET-EFDA, Culham Science Centre, Abingdon, OX14 3DB, UK

1) Ecole Polytechnique Fédérale de Lausanne (EPFL), Centre de Recherches en Physique des Plasmas (CRPP), Association EURATOM – Confédération Suisse, Lausanne, CH

2) EFDA-CSU, Culham Science Centre, Abingdon, UK

3) Institut de Recherche Astrophysique et Planétologie, Université de Toulouse – CNRS, FR

4) Culham Centre for Fusion Energy, Culham Science Centre, Abingdon, UK

5) Association Euratom – CEA, Cadarache, Saint-Paul-lez-Durance, FR

6) Oak Ridge National Laboratory, Fusion Energy Theory Group, Oak Ridge, USA

e-mail contact of corresponding author: duccio.testa@epfl.ch

Abstract. This paper reports on the results of recent experiments performed on the JET tokamak on Alfvén Eigenmodes (AEs) with toroidal mode number (n) in the range |n|=3-15. The stability properties of these medium-n AEs are investigated experimentally using a set of compact in-vessel antennas, providing a direct and real-time measurement of the frequency, damping rate and amplitude for each individual toroidal mode number. First, we describe the development of a new algorithm for real-time mode detection and discrimination using the Sparse Signal Representation theory. Second, we present measurements of the dependence of the damping rate for Toroidal AEs with $|n|\leq 8$ upon various background plasma parameters. Finally, the results of theoretical modeling of the damping rate for n=3 Toroidal AEs, performed with the LEMan, CASTOR and TAEFL codes, are shown as function of the edge plasma elongation.

1. Introduction and Background: the JET Alfvén Eigenmodes Diagnostic System.

The stability of Alfvén Eigenmodes (AEs) and the effect of these modes on the energy and spatial distribution of fast ions, including fusion generated αs, are among the most important physics issues for the operation of burning plasma experiments such as ITER. Of particular interest are AEs with toroidal mode number (n) in the range |n|~3-20, as these are expected to interact most strongly with the αs. The stability of these modes is investigated experimentally in JET using an active system (the so-called Alfvén Eigenmodes Active Diagnostic, AEAD)

*Appendix of F.Romanelli et al., Proceedings 23rd IAEA Fusion Energy Conference 2010, Daejeon, Korea.

based on a set of eight compact in-vessel antennas and real-time detection and discrimination of the individual n-components in the measured magnetic spectrum $|\omega\delta B_{MEAS}|(n)$ [1-3]. The AEAD system can now provide in real-time a direct measurement of the damping rate (γ/ω) during the dynamical evolution of the background plasma parameters, separately for all the antenna-driven toroidal mode numbers. The AEAD system consists principally of:

1. the AE exciter, built upon a function generator and a high-power amplifier connected to a set of up to eight in-vessel antennas, whose aim is to drive a very small magnetic perturbation, $\max(|\delta B_{DRIVEN}|)\sim 0.1$G at the plasma edge, i.e. 10^5 times smaller than the typical value of the toroidal magnetic field in JET, $B_{TOR}\sim(1\text{-}3)$T;
2. a receiver, built upon synchronous detection units, which collects signals from various in-vessel detectors (magnetic pick-up coils, electron cyclotron emission, reflectometry); this receiver is also connected to the real-time AE Local Manager (AELM) to allow the detection and tracking of antenna-driven plasma resonances with different toroidal mode numbers.

The antennas are installed in two groups of four closely-spaced units at two toroidally opposite positions, at the same poloidal location. Any combination of these eight antennas can be chosen with a ± relative phasing. Hence, as shown in fig1, a very broad toroidal spectrum is excited for any antenna frequency, comprising many components up to $|n|\sim 30$, of which the higher-n ones are more strongly attenuated as the distance from the antennas increases.

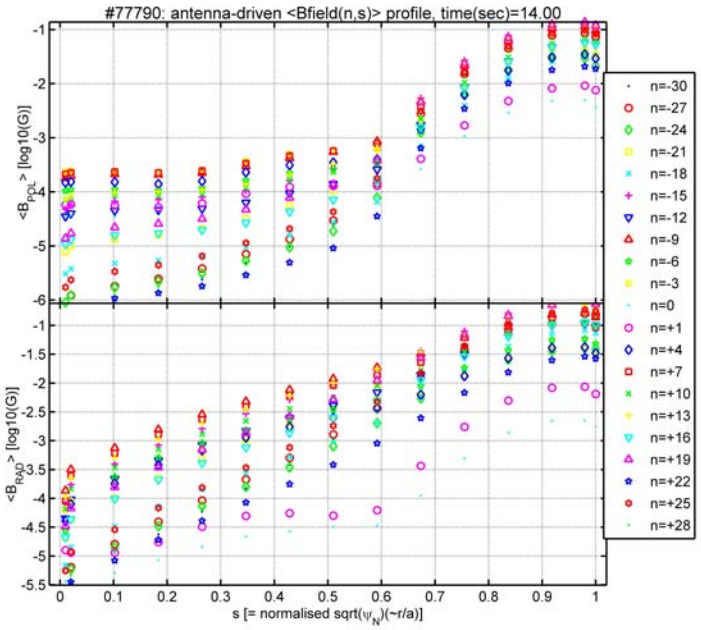

***Figure1**. An example of the antenna-driven, flux-surface averaged, radial ($<B_{RAD}(n,s)>$) and poloidal ($<B_{POL}(n,s)>$) magnetic field for the discharge #77790 at time=14.00sec for different n-components as function of the flux-surface label $s=\sqrt{\psi_N(r)}$, where $\psi_N(r)$ is the poloidal flux normalized to its value at the plasma edge (r=a).*

Note that up to two orders of magnitude difference in the antenna-driven magnetic field is seen between its different n-components up to $|n|\leq 30$, which makes it an essential requirement to be able to discriminate in real-time the different components in the measured $|\omega\delta B_{MEAS}|(n)$

spectrum. This observation has motivated the development of a novel method for mode detection and n-number discrimination using the Sparse Signal Representation theory and the SparSpec algorithm [4, 5], which has now been fully implemented in the AELM [6, 7]. The speed and accuracy of this algorithm makes it possible to use it in our plant control software, allowing the real-time tracking of many individual modes during the evolution of the plasma background, on a 1ms time scale. An example of this real-time detection and discrimination for the concurrent Toroidal AEs (TAEs) with $3 \le |n| \le 8$ is shown in fig2 for discharge #77788, where the excitation system was configured to drive predominantly n-odd modes, with $\max(|\delta B_{DRIVEN}(n)|)$ in the range $|n| \sim 3\text{-}7$, and producing a negligible drive for components with $|n| > 10$. Not only components with different n, but positive and negative n-components, with the same |n|, can be discriminated in real-time with our algorithm within a CPU-time of <850μs.

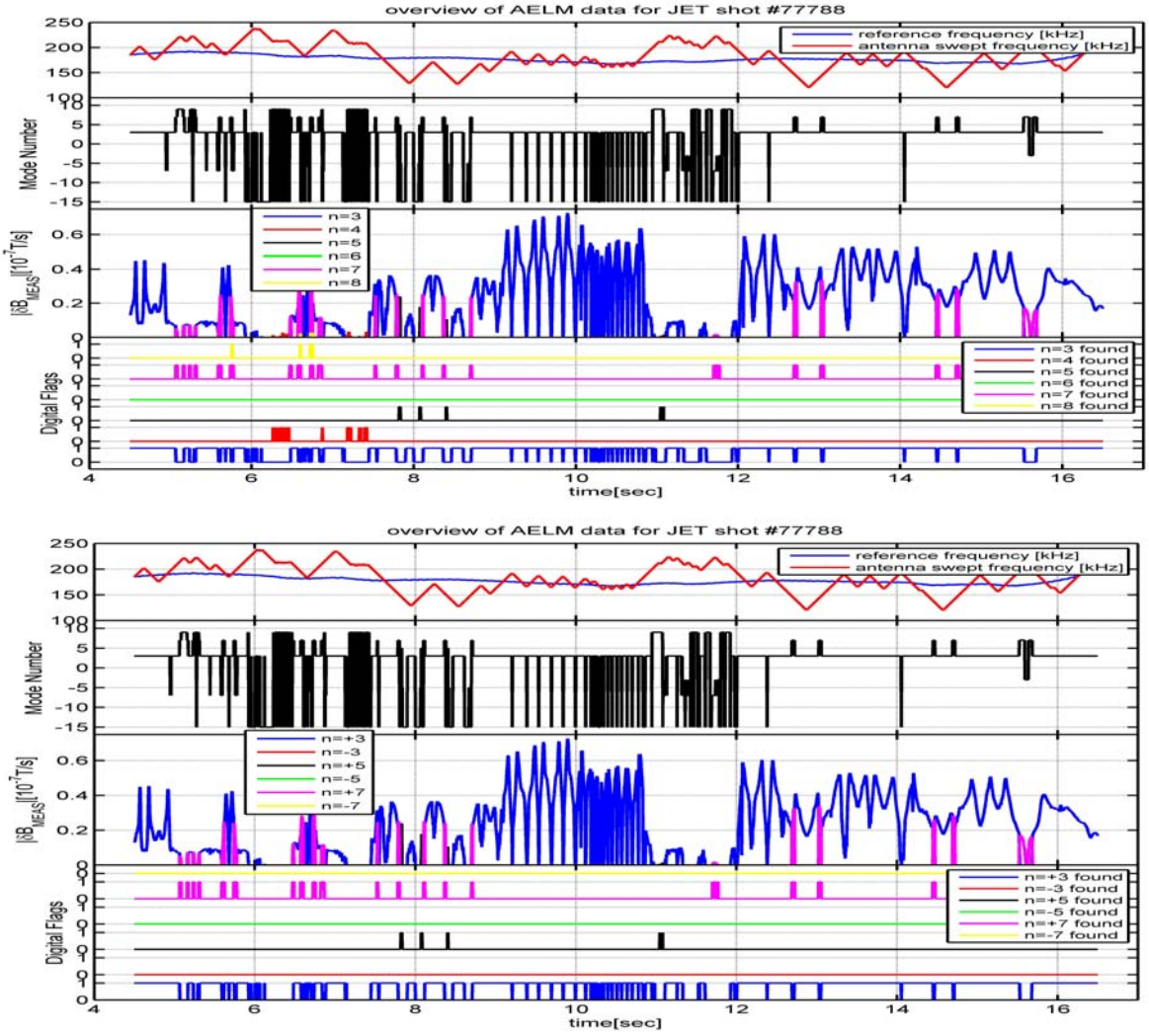

***Figure2**. Real-time discrimination between the different components in the antenna-driven AE spectrum for shot #77788; the calculation is performed using a CPU-time of <850μs; if high (=1), the digital signals (bottom frames) indicate successful detection of that n-component.*

2. Measurements of the Damping Rate for Medium-n Alfvén Eigenmodes in JET.

The measurements of the frequency and damping rate of medium-n AEs are routinely obtained in different JET operating scenarios [3, 8, 9]. An example is shown in fig3 for discharge #77417, where the AEAD system was configured to drive an odd-n spectrum peaked towards |n|=3-9, with a negligible drive for |n|>10 and |n|<3. The damping rate can be measured independently for many different n-components in a single discharge as the plasma background evolves, thanks to the successful implementation and exploitation of our innovative real-time mode discrimination and tracking algorithm.

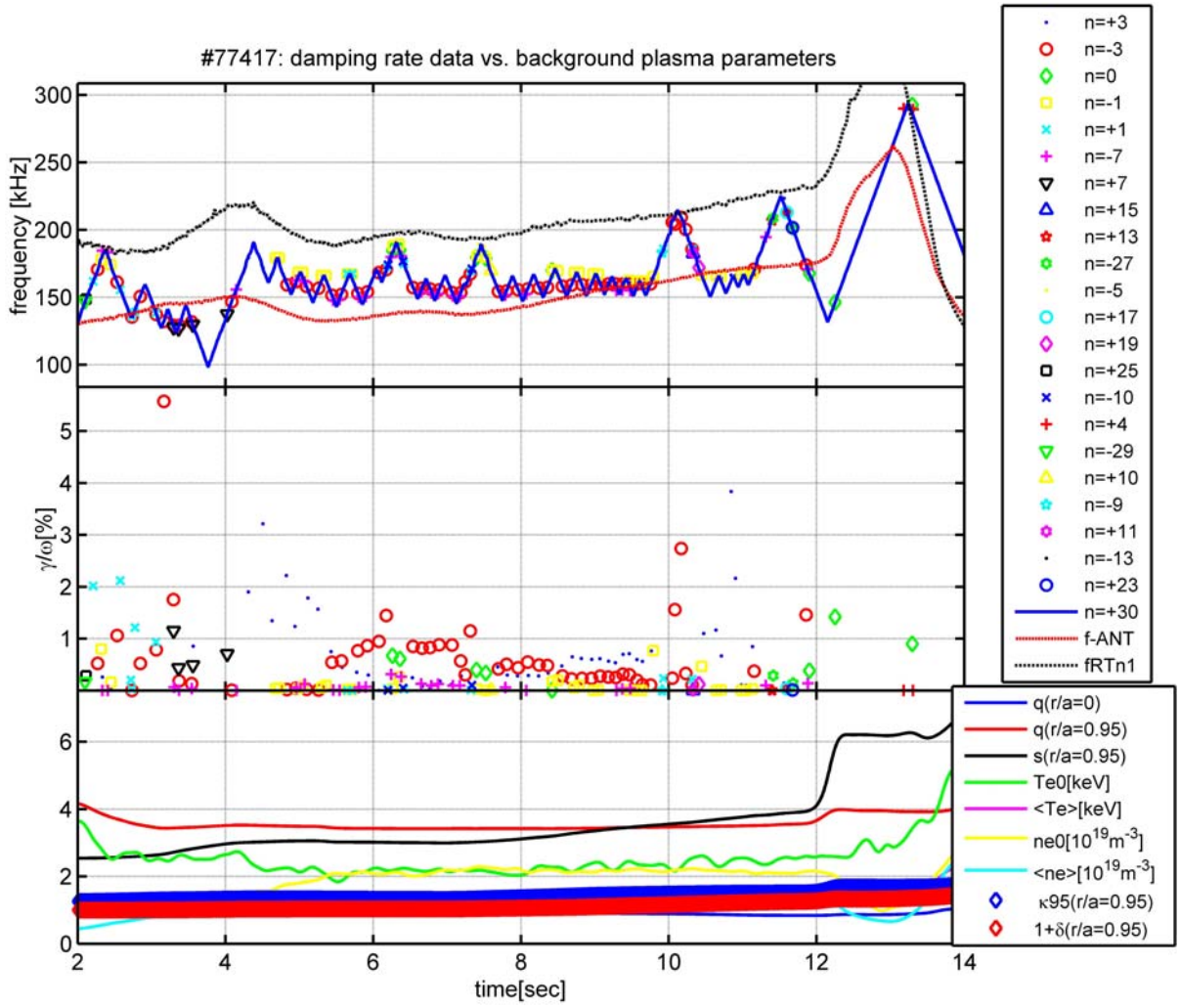

Figure3*. Measurement of the damping rate for individual toroidal mode numbers for the discharge #77417 as function of the evolution of the main background plasma parameters.*

Due to the large number of available data-points, and the subtle differences between different discharges, it is also clear from fig3 that two different approaches need to be used to analyze the dependence of γ/ω(n) upon background plasma parameters. First, we use a database approach, assembling the data for many different discharges [10]: this allows us to identify

the main dependencies of $\gamma/\omega(n)$, but also generates a large scatter in the processed data, due to the very sensitive dependence of $\gamma/\omega(n)$ on the details of the plasma profiles. Second, we compare selected discharges on a one-to-one basis [11]: this allows understanding how subtle differences in the background plasma profiles affect the measured $\gamma/\omega(n)$.

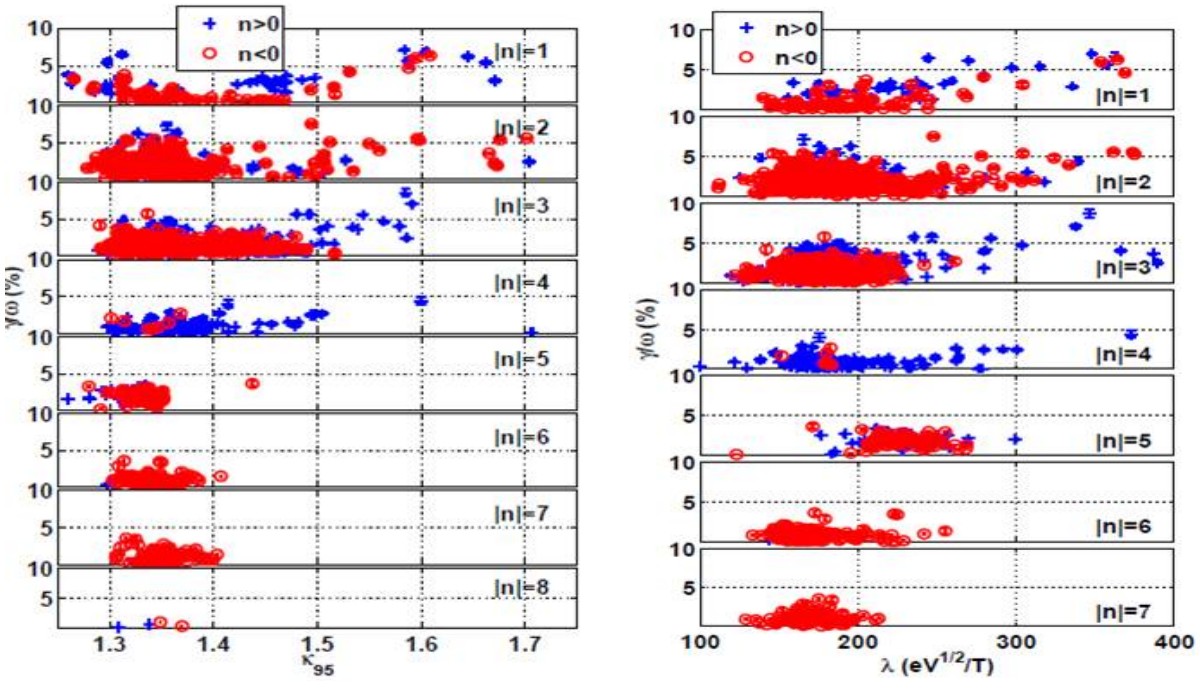

Figure4. *Database approach used to study the dependence of the measured $\gamma/\omega(n)$ vs. the edge elongation κ_{95} (up to $|n|\leq 8$) and the kinetic parameter λ (up to $|n|\leq 7$).*

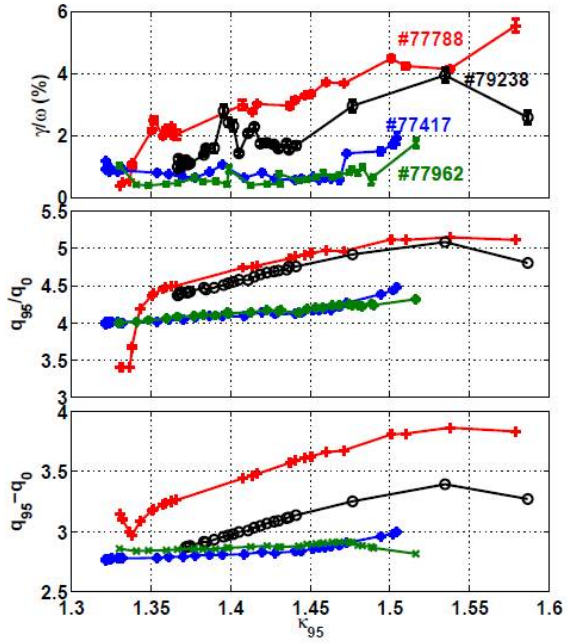

Figure5. *The measured $\gamma/\omega(n)$ increases with q_{95}/q_0 and q_{95}-q_0 for the same κ_{95}; this experimental trend is consistent with the theoretical scaling for the electron Landau damping $(\gamma/\omega)_{ELD} \propto n^2(q_{95}-q_0)^2$ and with the LEMan modeling for #77788 [8] (where damping of a n=3 TAE occurs mostly via mode conversion to Kinetic Alfvén Waves, then damped by electron Landau damping).*

Two examples of these studies are shown in fig4 for the study of $\gamma/\omega(n,\kappa_{95})$ and $\gamma/\omega(n,\lambda)$, where κ_{95} is the edge elongation and $\lambda \propto (sdq/ds)_{95}\sqrt{T_{e0}}/B_0$ provides for a simple qualitative

estimate of the radiative damping mechanism [12]. Regarding the $\gamma/\omega(n,\kappa_{95})$ dependence, we note that the maximum value of κ_{95} for which $\gamma/\omega(n)<7\%$ can be measured highlights a strong effect of the edge shape on the damping rate for medium-n TAEs, which could be used for real-time control purposes. Regarding the $\gamma/\omega(n,\lambda)$ dependence, we note a very clear trend for $|n|=1$: $\gamma/\omega(|n|=1)\propto 0.77\times\lambda$, a similar trend for $2\leq|n|\leq4$, but only for large $\lambda>250[\sqrt{eV}/T]$, whereas no clear trend is observed for $|n|\geq5$. Figure5 then shows the comparison of $\gamma/\omega(\kappa_{95}(t))$ for n=3 TAEs for four different discharges, where $\kappa_{95}(t)$ was very similar, but we had a different time evolution of the safety factor q(t). We note that the differences in γ/ω for the same κ_{95} and n=3 in these four different discharges correlate very well with q_{95}/q_0 and $q_{95}-q_0$.

3. Modeling of the Damping Rate of n=3 Toroidal Alfvén Eigenmodes.

In JET, the edge plasma shape and magnetic shear have been found to be key ingredients for increasing the damping rate of both antenna-driven, low-n (n=1, n=2) [13] and fast-ion driven, medium-n (n~3-10) [14] TAEs. This has motivated experimental studies on the Alcator C-mod tokamak where it was found that the damping rate of an n=6 TAE remains essentially invariant when the average edge triangularity (δ_{95}) is varied in the range $0.3<\delta_{95}<0.7$ [15]. Conversely, the data obtained for the n=3 and n=7 TAEs during the two otherwise similar JET discharges presented in fig6 show an almost linear increase of the damping rate as a function of the edge elongation κ_{95}. In fact, as edge elongation increases, an even stronger increase in the damping rate for n=3 and n=7 TAEs is observed than for n=1 and n=2 TAEs, with this trend having been confirmed across the n-spectrum up to at least n=7.

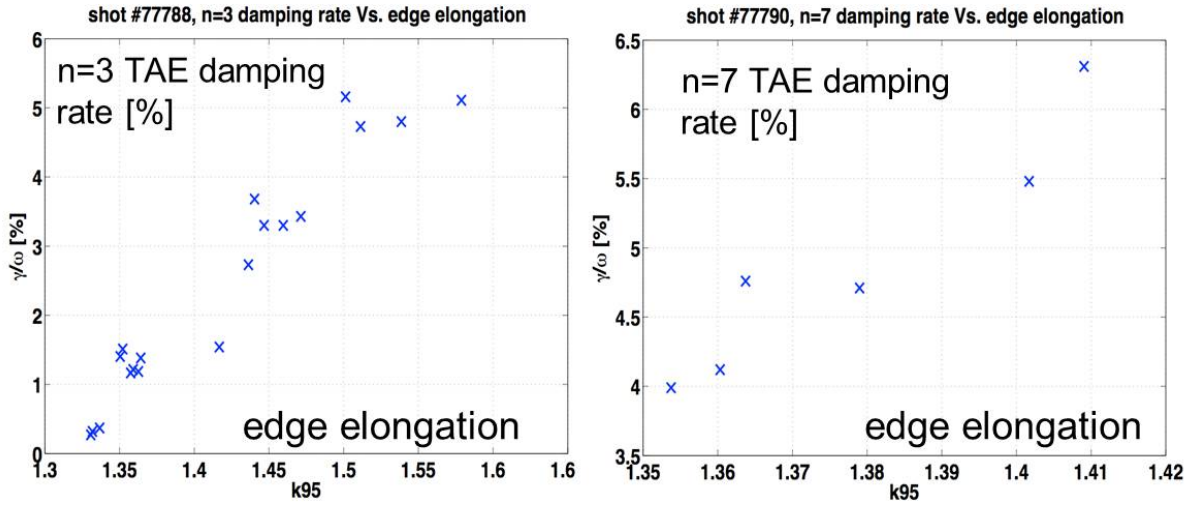

Figure6*. The measured damping rate for n=3 and n=7 TAEs vs. the edge elongation κ_{95} for the two otherwise similar discharges #77788 and #77790.*

The discharge #77788 has been used for detailed comparisons with theory and models in the framework of the ITPA activities [16]. Figure7 shows the damping rate for n=3 TAEs as a function of the edge elongation in ohmic plasmas together with the results of simulations performed with the LEMan [17, 18], TAEFL [19, 20] and CASTOR [21] codes. Both the LEMan and the TAEFL codes model the actual plasma shape using a magnetic configuration which is up/down symmetric, but non-circular.

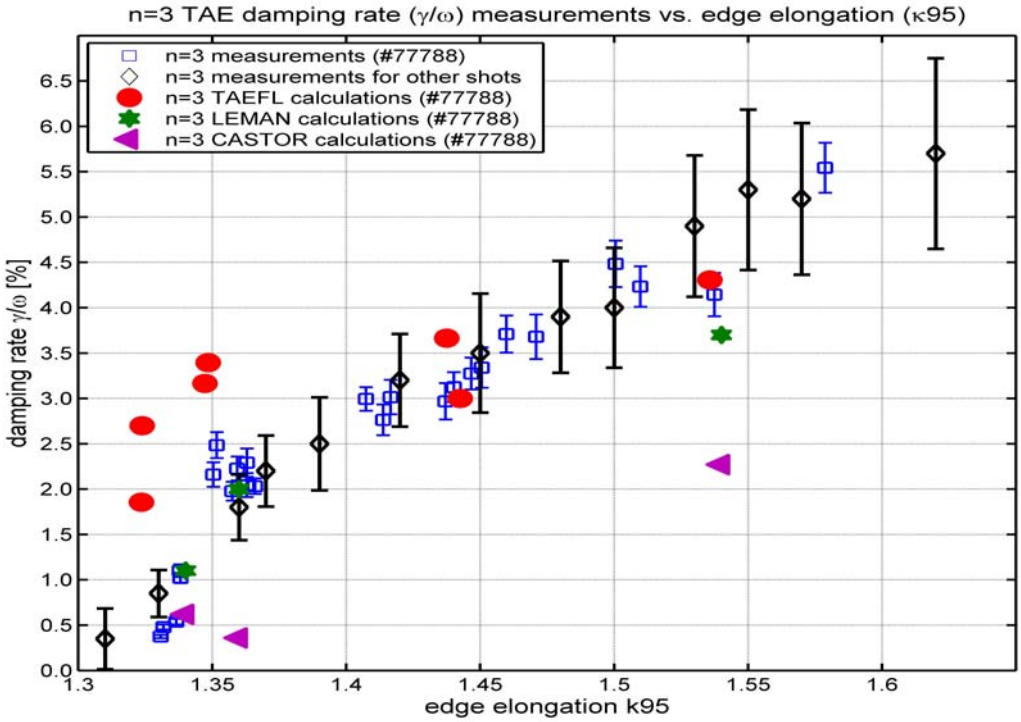

Figure7*. Damping rate data for the n=3 TAE as function of* κ_{95}*, showing a linear dependence* $\gamma/\omega=f(\kappa_{95})$*, compared with the results of the LEMan, TAEFL and CASTOR simulations.*

First, it is important to note that, despite the differences between the codes, the radial Eigenfunctions computed by CASTOR, TAEFL and LEMan are in sufficiently good agreement between each other, indicating a good understanding of the physics mechanisms contributing to determining the stability of these medium-n AEs, and of the effect that the differences between the various codes and models can have on the predictions for ITER [16].

The LEMan results [8] show that the mode frequency and damping rate are in rather good agreement with the measurements (mode frequency within 10%, damping rate within ~50%), this exercise also demonstrating that a rather large number of poloidal harmonics needs to be used to reproduce quantitatively the measured γ/ω even for moderately low-n modes.

The TAEFL code is a reduced MHD initial value code that uses gyrofluid closure techniques for the energetic ions to incorporate the Landau resonance effects that destabilize Alfvén

modes. Since only unstable modes can be analyzed by TAEFL, the technique used was to start with an unstable Alfvén mode, vary the fast ion drive and extrapolate back to zero drive in order to determine an effective damping rate. Fast ion profiles/parameters are chosen that lead to a mode very close to the frequency excited by the antenna. This model incorporates ion/electron Landau damping, continuum damping and radiative damping (due to finite ion Larmor radius) effects. It uses Fourier spectral representations in the poloidal and toroidal directions and finite differences in the direction normal to the flux surfaces. The TAEFL simulations of JET plasmas used 300-400 radial points and 26 Fourier modes (m=0→25). The TAEFL results [9] are in very good agreement with the measurements for relative high values of the elongation (κ_{95}>1.45), whereas the discrepancy at lower values of κ_{95} is larger.

The CASTOR calculations used 11 poloidal harmonics (m=3→13), the resistivity was set to $\eta=1\times10^{-7}$, and the radial extent was set to s=0→0.95. The CASTOR code correctly predicts the mode frequency, whereas the large discrepancy with the measured damping rate can be due to small uncertainties in the q- and/or density profiles, and to the absence of kinetic effects. For instance, slightly different values of q- or density at s~0.55 can make the mode intersect the continuum and increase γ/ω_{CASTOR} by a factor of 2. In addition to this, kinetic effects such as radiative and Landau damping have been shown to play an important role with other codes such as LEMan and LIGKA [22]. Hence continuum damping, which is the only mechanism included in CASTOR simulations, can only account for a fraction of the measured γ/ω, indicating that other mechanisms make important contributions to the total damping.

4. Conclusions.

A new algorithm, based on the Sparse Representation of signals, has been developed and fully implemented to discriminate in real-time the different toroidal components in the plasma response to the multi-components, frequency-degenerate, magnetic field spectrum driven by the AE antennas in JET. The quantitative analysis of damping rate measurements obtained in JET for n=3 and n=7 TAEs has confirmed that γ/ω increases as the edge elongation (hence the edge magnetic shear) is increased. This scaling agrees with previous JET data for low-n TAEs, and with theoretical estimates based on mode conversion of TAEs to Kinetic Alfvén Waves. These new JET experimental results further confirm the possibility of using the edge shape parameters as a real-time actuator for the control of the AE stability in burning plasma experiments. Detailed simulations performed with the LEMan, TAEFL and CASTOR codes have demonstrated that our general understanding of the AE stability properties is reaching a

good quantitative level, and in particular that we need to include in the calculations a large number of poloidal harmonics, and that continuum damping is not the only mechanism accounting for the measured damping rate for these modes.

References.

1. Fasoli, A., et al., Phys. Rev. Lett. **75** (1995), 645.
2. Testa, D., et al., "The new Alfvén Wave Active Excitation System at JET", Proceedings 23rd SOFT Conference (2004); weblink: http://infoscience.epfl.ch/record/143354/files/.
3. Panis, T., Testa, D. et al., Nucl. Fusion **50** (2010), 084019.
4. Bourguignon, S., Carfantan, H., Böhm, T., Astronomy and Astrophysics **462** (2007), 379.
5. Klein, A., Carfantan, H., Testa, D. et al., Plasma Phys. Control. Fusion **50** (2008), 125005.
6. Testa, D., et al., Fusion Engineering and Design **86** (2011), 381.
7. Testa, D., et al., Europhysics Letters **92** (2010), 50001.
8. Testa, D., et al., Nucl. Fusion **50** (2010), 084010.
9. Testa, D., et al., Nucl. Fusion **51** (2011), 043009.
10. Panis, T., et al., *Analysis of damping rate measurements of toroidal Alfvén Eigenmodes on JET as a function of n, part-I: database approach*, to be submitted to Nuclear Fusion.
11. Panis, T., et al., *Analysis of damping rate measurements of toroidal Alfvén Eigenmodes on JET as a function of n, part-II: discharge comparison*, to be submitted to Nuclear Fusion.
12. C.Cheng, Phys. Rep. **211** (1992), 1.
13. Testa, D., and Fasoli, A., Nucl. Fusion **41** (2001), 809.
14. Testa, D., Fasoli, A., Borba, D., et al., Plasma Phys. Control. Fusion **46** (2004), S59.
15. Snipes, J.A., Basse, N., Boswell, C., et al., Phys. Plasmas **12** (2005), 056102.
16. Lauber. Ph., et al., paper THW/P7-08, IAEA-FEC 2010.
17. Popovich, P., Cooper W.A., Villard, L., Comput. Phys. Comm. **175** (2006), 250.
18. Mellet, N., Cooper, W.A., Popovich, P., Villard, L., Brunner, S., Comp. Phys. Comm. **182** (2011), 570.
19. Spong, D.A., Carreras, B.A., and Hedrick, C.L., Phys. Fluids **B4** (1992), 3316.
20. Spong, D.A., Carreras, B.A., and Hedrick, C.L., Phys. Plasmas **1** (1994), 1503.
21. Kerner, W., Goedbloed, J.P., et al., Journal of Computational Physics **142** (1998), 271.
22. Lauber, Ph., Günter, S., et al., Journal of Computational Physics **226** (2007), 447.

Acknowledgements.

This work was supported by EURATOM under the contract of Association with CRPP-EPFL, and was carried out within the framework of the European Fusion Development Agreement. This work was also partly supported by the Swiss National Science Foundation. The views and opinions expressed herein do not necessarily reflect those of the European Commission. The Authors would like to thank the various members of the CRPP, MIT and JET staff that contributed to the design, installation, commissioning and operation of the TAE antenna system.